# Synthesis and Tissue Biodistribution of [ω-$^{11}$C]Palmitic Acid. A Novel PET Imaging Agent for Cardiac Fatty Acid Metabolism[1]

Brad O. Buckman,[†] Henry F. VanBrocklin,[†,‡] Carmen S. Dence,[§] Steven R. Bergmann,[⊥] Michael J. Welch,[§] and John A. Katzenellenbogen*[,†]

*Department of Chemistry, University of Illinois, 600 South Mathews Avenue, Urbana, Illinois 61801, Mallinckrodt Institute of Radiology, Washington University School of Medicine, 510 South Kingshighway, St. Louis, Missouri 63110, and Department of Internal Medicine, Cardiovascular Division, Washington University School of Medicine, 660 South Euclid Avenue, St. Louis, Missouri 63110*

*Received March 2, 1994*[⊗]

In order to diagnose patients with medium-chain acyl-CoA dehydrogenase deficiency with a noninvasive diagnostic technique such as positron emission tomography, we have developed a synthesis of [ω-$^{11}$C]palmitic acid. The radiochemical synthesis was achieved by coupling an alkylfuran Grignard reagent (**7**) with [$^{11}$C]methyl iodide, followed by rapid oxidative cleavage of the furan ring to the carboxylate using ruthenium tetraoxide. Tissue biodistribution studies in rats comparing [ω-$^{11}$C]palmitic acid and [1-$^{11}$C]palmitic acid show that the %ID/g and %ID/organ in the heart tissue after administration of [ω-$^{11}$C]palmitic acid is approximately 50% greater than after administration of [1-$^{11}$C]palmitic acid, due to the diminished metabolism of the [ω-$^{11}$C]palmitic acid. These studies show as well, low uptake in nontarget tissues (blood, lung, kidney, and muscle). PET images of a dog heart obtained after administration of [ω-$^{11}$C]- and [1-$^{11}$C]palmitic acid show virtually identical uptake and distribution in the myocardium. The differing cardiac washout of labeled palmitates measured by dynamic PET studies may allow diagnosis of disorders in cardiac fatty acid metabolism.

## Introduction

Under normal physiological conditions, oxidation of fatty acids provides the major source of energy for the heart. The initial step in each cycle of β-oxidation is catalyzed by a family of acyl-CoA dehydrogenases, the members of which are specific for certain fatty acid chain lengths. Genetic defects in the β-oxidation pathway are recognized as important causes of hypoketotic hypoglycemia, cardiomyopathy, skeletal myopathy, and sudden death in children.[2a–e] Patients with either medium- or long-chain acyl-CoA dehydrogenase deficiencies (MCAD or LCAD deficiencies) exhibit the inability to metabolize fatty acids of certain chain lengths effectively. For example, patients with medium-chain acyl-CoA dehydrogenase deficiency are unable to metabolize fatty acids containing 6–12 carbons. The increase in fatty acid intermediates (specifically acylcarnitine species) that occur in these deficiencies may be arrythmogenic in these patients and lead to sudden cardiac death, especially during conditions such as fasting. Currently, there is no diagnostic method to evaluate the cardiac metabolism in these patients, nor to predict the severity of their biochemical abnormality.[2b,c] Thus, a noninvasive diagnostic method that can detect defects of fatty acid oxidation in the heart in vivo is needed.

Positron emission tomography (PET), a noninvasive technique used to image biochemical processes,[3] requires physiologically active ligands labeled with short-lived positron-emitting radioisotopes, such as carbon-11, fluorine-18, oxygen-15, and nitrogen-13, to target the area of interest. Imaging agents such as 2-[$^{18}$F]fluorodeoxyglucose, [1-$^{11}$C]palmitate, and [1-$^{11}$C]acetate are commonly used to examine myocardial metabolism by PET and, through physiological-based mathematical models, to delineate specific metabolic pathways and their perturbations.[3] Fatty acid-based radiopharmaceuticals which are labeled with fluorine-18 or iodine-123, or contain other steric or functional perturbations of the fatty acid structure (e.g., β-methyl substitution), may not be metabolized as their natural analogues and thus may give misleading results.[4] As a result, the fatty acids themselves, with simple carbon-11 isotopic substitution, are likely to be the most effective radiotracers to probe certain details of cardiac metabolism.

Previous studies have demonstrated that [1-$^{11}$C]-palmitate can be used to delineate oxidation abnormalities in patients with inherited deficiencies of long-chain acyl-CoA dehydrogenase.[2c] However, since the C-1 carbon is cleaved in the initial step of β-oxidation, patients with medium- or short-chain dehydrogenase deficiencies would be expected to show normal kinetics in the myocardial handling of long-chain fatty acids labeled in the C-1 position. We hypothesized that by labeling palmitic acid at the ω-position, the initial β-oxidation steps to shorter chain lengths will occur in an unhampered fashion. However, when the carbon chain is degraded to the length where it becomes a substrate for the enzyme that is impaired, the kinetics of further tracer metabolism will be reduced, so the ultimate release of the ω-carbon as [$^{11}$C]carbon dioxide should be retarded. Simpler, shorter chain fatty acids which might be used to study specific enzyme deficien-

* Address correspondence to: Professor John A. Katzenellenbogen, Department of Chemistry, University of Illinois, Box 37 Roger Adams Laboratory, 600 S. Mathews Avenue, Urbana, IL 61801. KATZENELL@UIUCSCS (Bitnet). KATZENELL@B.SCS.UIUC.EDU (Internet).

† Department of Chemistry, University of Illinois.

‡ Present address: Center for Functional Imaging, Lawrence Berkeley Laboratory, 1 Cyclotron Rd., Berkeley, CA 94720.

§ Mallinckrodt Institute of Radiology, Washington University School of Medicine.

⊥ Department of Internal Medicine, Cardiovascular Division, Washington University School of Medicine.

⊗ Abstract published in *Advance ACS Abstracts,* June 15, 1994.

0022-2623/94/1837-2481$04.50/0 

**Scheme 1**

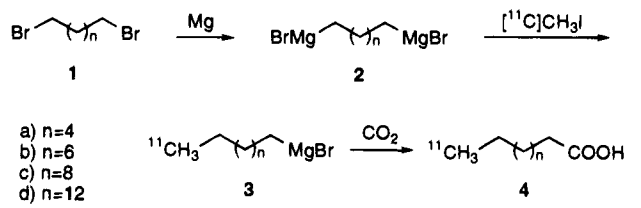


**Scheme 2**

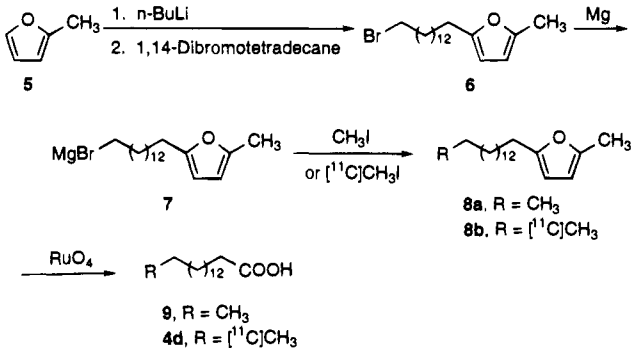


cies are not viable targets, since they are poorly extracted into the myocardium.

Recently, a synthesis of [$\omega$-$^{11}$C]-labeled hexanoic (**4a**), octanoic (**4b**), and decanoic (**4c**) acids has been described using $\alpha,\omega$-bis-Grignard reagent **2**, which was coupled with [$^{11}$C]methyl iodide at one terminus, followed by reaction with carbon dioxide at the opposite end (Scheme 1).[5] Preparing [$\omega$-$^{11}$C]palmitic acid via this method would require generation of bis-Grignard reagent **2d** and its conversion to **4d**.

The radiosynthetic strategy we develop in this report obviates the need for the potentially unstable tetradecane bis-Grignard reagent **2d** and the two distinct carbon–carbon bond forming steps (**2** to **4**), which might produce unwanted carbon-11 labeled products. As an alternative, we envisaged that the reactive carboxylate could be present in latent form as a furan ring, from which it could be rapidly unmasked in the last step by oxidative cleavage. Thus, alkyl furan mono-Grignard reagent **7** was prepared and coupled with [$^{11}$C]methyl iodide; rapid oxidative cleavage using catalytic ruthenium tetraoxide[6] gave [$\omega$-$^{11}$C]palmitic acid (4d) (Scheme 2). This rapid oxidation is well-suited for use in radiochemical synthesis with short-lived radionuclides such as carbon-11 ($t_{1/2}$ = 20.4 min).

## Results and Discussion

**Chemical and Radiochemical Synthesis.** The Grignard precursor **6** was formed by ortho-lithiation of 2-methylfuran (**5**) with *n*-BuLi, followed by alkylation[7] with 1,14-dibromotetradecane to provide (bromoalkyl)-furan **6** in 67% yield (Scheme 2). 2-Methylfuran was chosen over furan to preclude removal of the second acidic proton $\alpha$ to the oxygen. Efficient formation of Grignard reagent **7** was not achieved without considerable experimentation: acceleration of the sluggish reaction of bromide **6** with magnesium in THF at 30 °C by entrainment with 1,2-dibromoethane at 60 °C gave side products derived from elimination (**11**), dimer formation (**13**), and reaction with oxygen (**12**);[8,9] reaction of bromide **6** with activated Rieke magnesium[10] minimized elimination but not dimer formation. Finally, addition of bromide **6** over 3 h via syringe pump to magnesium with a trace of iodine in THF at 35 °C provided pure solutions of Grignard reagent **7**.

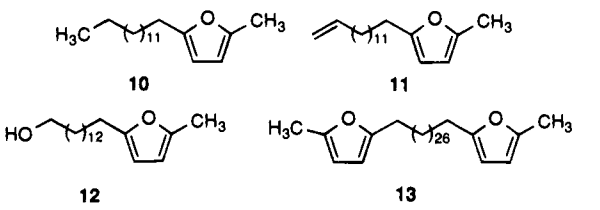


In a model study, Grignard reagent **7** was coupled with methyl iodide in the presence of $Li_2CuCl_4$ to afford the alkylated product **8a**.[11] Oxidative cleavage with sodium periodate and catalytic ruthenium trichloride gave palmitic acid (**9**) in 97% yield. Our homogeneous tetrahydrofuran–water–acetonitrile solvent system worked as well as the biphasic system described by Sharpless.[6]

[$^{11}$C]Methyl iodide, prepared from [$^{11}$C]carbon dioxide as previously described,[12] was distilled in a stream of nitrogen through a trap filled with NaOH pellets and $P_2O_5$ powder to remove unwanted [$^{11}$C]carbon dioxide, hydrogen iodide, and water. The [$^{11}$C]methyl iodide was then trapped in tetrahydrofuran at 0 °C, and the Grignard reagent **7** was added to produce the methylated species **8b**. The minimum concentration of Grignard reagent **7** that was required to give >90% incorporation of carbon-11 was 0.13 M (0.21 mmol). This is a relatively high concentration, and it suggests that some of the organometallic species is being protonated to form alkylfuran **10**; it also indicates that the removal of water or hydrogen iodide during the preparation of [$^{11}$C]methyl iodide, despite our precautions, is incomplete. The addition of $Li_2CuCl_4$ had no effect on the levels of carbon-11 incorporation and thus was not used in the radiochemical synthesis. Labeled furan **8b** was oxidatively cleaved in 8 min with sodium periodate and catalytic ruthenium trichloride. Darkly-colored material and ruthenium dioxide were rapidly removed from the reaction mixture by chromatography through Chelex 100 resin and silica gel with pentane as eluent.

After oxidation, any alkylfuran **10** derived from protonolysis of unreacted Grignard reagent **7** would have been cleaved to unlabeled pentadecanoic acid. We did not expect the non-naturally occurring pentadecanoic acid to interfere with the subsequent biological evaluation of the labeled palmitic acid, since the mass of the dose injected would not appreciably increase the amount of endogenous fatty acid in the blood. Finally, incubation with human serum albumin (HSA)[13] provided [$\omega$-$^{11}$C]palmitic acid (**4d**) in an injectable form suitable for biological investigation in under 75 min of total synthesis time. The unbound [$\omega$-$^{11}$C]palmitic acid, [1-$^{11}$C]palmitic acid, and palmitic acid itself have identical HPLC retention times; the [$\omega$-$^{11}$C]palmitic acid–HSA complex and the [1-$^{11}$C]palmitic acid–HSA complex also have identical HPLC retention times.

**Biological Investigation.** For animal tissue biodistribution studies, [$\omega$-$^{11}$C]palmitic acid bound to HSA was injected intravenously into female Sprague–Dawley rats (140–160 g, four rats per time point). Following 5-, 10-, 15-, 30-, and 60-min intervals, the rats were sacrificed and the tissue biodistribution was determined. The distributions of [$\omega$-$^{11}$C]palmitic acid (**4d**) and, for

**Table 1.** Biodistribution Data for [1-$^{11}$C]Palmitic Acid

| | %ID/g | | | | |
|---|---|---|---|---|---|
| | 5 min | 10 min | 15 min | 30 min | 1 h |
| blood | 0.116 ± 0.019 | 0.130 ± 0.033 | 0.373 ± 0.189 | 0.329 ± 0.048 | 0.157 ± 0.020 |
| lung | 0.945 ± 0.414 | 1.272 ± 0.203 | 1.246 ± 0.480 | 1.173 ± 0.177 | 1.080 ± 0.149 |
| liver | 5.941 ± 2.013 | 8.361 ± 1.474 | 6.252 ± 2.751 | 5.623 ± 0.396 | 4.853 ± 0.184 |
| kidney | 0.994 ± 0.346 | 1.343 ± 0.147 | 1.184 ± 0.398 | 1.301 ± 0.212 | 1.238 ± 0.102 |
| muscle | 0.183 ± 0.079 | 0.179 ± 0.027 | 0.166 ± 0.040 | 0.198 ± 0.017 | 0.194 ± 0.022 |
| heart | 0.996 ± 0.340 | 1.080 ± 0.407 | 1.011 ± 0.520 | 0.941 ± 0.074 | 0.792 ± 0.217 |

**Table 2.** Biodistribution Data for [$\omega$-$^{11}$C]Palmitic Acid

| | %ID/g | | | | |
|---|---|---|---|---|---|
| | 5 min | 10 min | 15 min | 30 min | 1 h |
| blood | 0.250 ± 0.040 | 0.171 ± 0.006 | 0.310 ± 0.075 | 0.430 ± 0.125 | 0.237 ± 0.052 |
| lung | 1.353 ± 0.159 | 1.427 ± 0.241 | 1.165 ± 0.098 | 1.423 ± 0.255 | 1.154 ± 0.212 |
| liver | 8.189 ± 0.292 | 8.382 ± 0.469 | 8.195 ± 0.518 | 8.252 ± 1.035 | 6.944 ± 0.453 |
| kidney | 1.154 ± 0.102 | 1.184 ± 0.193 | 1.105 ± 0.087 | 1.280 ± 0.263 | 1.166 ± 0.269 |
| muscle | 0.197 ± 0.024 | 0.198 ± 0.041 | 0.221 ± 0.093 | 0.222 ± 0.090 | 0.237 ± 0.032 |
| heart | 1.675 ± 0.387 | 1.372 ± 0.211 | 0.981 ± 0.479 | 1.813 ± 0.626 | 1.159 ± 0.147 |

comparison, [1-$^{11}$C]palmitic acid are shown in Tables 1 and 2, respectively.

Both [$^{11}$C]palmitates show high uptake in the liver due to normal metabolic clearance and fairly low uptake in nontarget tissues (blood, lung, kidney, and muscle). Increased radioactivity in the liver, muscle, and lung can reduce the quality of myocardial PET images by decreasing image contrast. Importantly, neither the $\omega$-position of the radionuclide nor the macroscopic quantities of unlabeled, non-naturally occurring pentadecanoic acid in the preparation adversely affect the tissue biodistribution of [$\omega$-$^{11}$C]palmitic acid compared to [1-$^{11}$C]palmitic acid.

Gratifyingly, the uptake in the heart for both tracers is fairly high. In fact, the %ID/g in the heart tissue after administration of [$\omega$-$^{11}$C]palmitic acid is approximately 50% greater than after administration of [1-$^{11}$C]palmitic acid. It is unlikely that the *uptake* into the heart of [$\omega$-$^{11}$C]palmitic acid is greater than [1-$^{11}$C]palmitic acid. Accordingly, the higher initial levels of [$\omega$-$^{11}$C]palmitic acid in the heart tissue is likely due to the fact that the $\omega$-labeled carbon is retained to a greater extent than the C-1 labeled carbon. The label in [1-$^{11}$C]palmitic acid is rapidly oxidized to [$^{11}$C]carbon dioxide which leaves the heart; this process involves one round of $\beta$-oxidation to generate [1-$^{11}$C]acetate, which releases the label as [$^{11}$C]carbon dioxide after only one round of the tricarboxylic acid (TCA) cycle. By contrast, sequential two-carbon $\beta$-oxidative cleavage of [$\omega$-$^{11}$C]palmitic acid eventually generates, as a final two-carbon fragment, [2-$^{11}$C]acetate. The fate of the C-2 carbon in acetate is different from the C-1 carbon, as it is equilibrated between the two carbonyl groups in succinate in the TCA cycle and is only partially released in each subsequent turn of the cycle. Thus the C-2 carbon is more likely to be incorporated into amino acids,[14a-c] which may account for the prolonged myocardial retention of the extracted [$\omega$-$^{11}$C]palmitic acid.

To assess [$\omega$-$^{11}$C]palmitic acid (**4d**) as a cardiac PET imaging agent and as an in vivo diagnostic agent for cardiac fatty acid metabolism, we examined **4d** and, for comparison, [1-$^{11}$C]palmitic acid in an intact, normal dog. Figure 1 shows midventricular PET images of a dog heart under resting conditions after intravenous administration of the [$^{11}$C]palmitates. On the top row are composite images obtained after the administration of [$\omega$-$^{11}$C]palmitic acid, and on the bottom row are images obtained after the administration of [1-$^{11}$C]-palmitic acid in the same dog. These represent data taken from the first 90 s (left), from 3 to 8 min (middle), and from 10 to 20 min (right), and they show that the radiotracers initially predominate in the blood pool, followed by gradual accumulation of the radiotracers in the myocardium and concomitant clearance from the blood. The two radiotracers show virtually analogous uptake and distribution; however, no qualitative differences were expected, since the study was performed using a normal dog. The poorer quality of the images on the top row is likely due to the smaller amount of radioactivity administered.

In conclusion, we have completed the first synthesis of [$\omega$-$^{11}$C]palmitic acid by coupling alkylfuran **7** with [$^{11}$C]methyl iodide, followed by oxidative cleavage of the furan ring to the carboxylic acid. The rapid perruthenate oxidation is key to the success of this synthesis and should find further use in short-lived radiopharmaceutical synthesis. Tissue biodistribution studies in rats have shown that the metabolism of [$\omega$-$^{11}$C]palmitic acid is different from [1-$^{11}$C]palmitic acid. PET images of a dog heart obtained after administration of both [$\omega$-$^{11}$C] and [1-$^{11}$C]palmitic acid show virtually identical uptake and distribution in the myocardium. The differing cardiac washout of labeled fatty acids may allow in vivo diagnosis of medium- and short-chain acyl-CoA dehydrogenase deficiency by dynamic PET studies.

## Experimental Section

**General Methods.** $^1$H and $^{13}$C NMR spectra were obtained on Varian 200XL or a Varian Unity 400 spectrometer. Fast atom bombardment (FAB) mass spectra were obtained on VG ZAB-SE spectrometer, electron impact (EI) mass spectra were obtained on a Finnigan MAT CH5 instrument, and chemical ionization (CI) mass spectra were obtained on a VG-70-SE-4F instrument. Elemental analysis was performed by University of Illinois microanalytical lab. Gas chromatograms were run using an HP 5790A with an HP Ultra 1 (cross linked methyl silicone gum) column, an FID detector, and the following temperature program: 150 °C for 2 min, 10 °C/min to 280 °C, 280 °C for 10 min. HPLC for the radiochemical experiments was performed on a Spectra-Physics 8700 chromatograph equipped with a UV detector (operating at 215 nm) and a NaI(Tl) radioactivity detector.

**2-(14-Bromotetradecyl)-5-methylfuran (6).** To a solution of 2-methylfuran (0.93 g, 11.4 mmol) in 10 mL of THF at

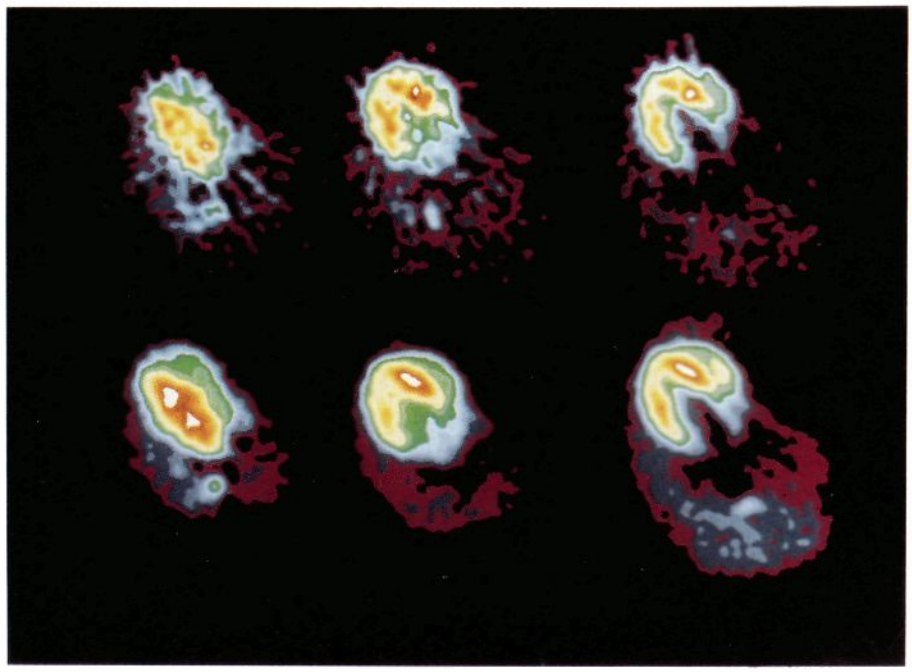

**Figure 1.** Single midventricular PET images of a dog heart after administration of [$\omega$-$^{11}$C]palmitic acid (top) and [1-$^{11}$C]palmitic acid (bottom). For orientation of the image, the left is the lateral free wall, 11 to 1 o'clock is the anterior myocardium, 1 to 4 o'clock is the septum, and posterior represents the mitral valve plane which is not visualized.

−20 °C was added *n*-butyllithium (5.9 mL of 1.6 M, 9.5 mmol). The solution was stirred for 0.5 h warmed to 0 °C for an additional 0.5 h, at which time 1,14-dibromotetradecane (5.07 g, 14.3 mmol) in 5 mL of THF was added. The mixture was allowed to warm to room temperature overnight and then quenched in 10% aqueous HCl. The aqueous layer was extracted with ether, and the combined organic layers were washed with 10% HCl and saturated $NaHCO_3$ and dried over $MgSO_4$. Evaporation in vacuo afforded crude **6.** Flash chromatography on silica gel (hexanes) afforded pure 2.16 g (67%) pure **6**: $^1$H NMR (200 MHz) 1.39−1.21 (m, 24 H), 1.61 (m, 2 H), 1.85 (p, 2 H, $J$ = 7.4), 2.55 (t, 2 H, $J$ = 7.0), 3.40 (t, 2 H, $J$ = 6.8), 5.89 (s, 2 H); $^{13}$C NMR 154.8, 150.0, 105.7, 105.0, 34.1, 32.8, 29.6 (5), 29.4, 29.3, 29.2, 28.8, 28.2, 28.1, 28.0, 13.5; IR (neat) 2910, 2870, 1570, 1460, 1210, 1020, 770; EIMS (70 eV) 358, 356 ($M^+$, 16), 95 (100); GC $t_R$ 6.71 min. Anal. ($C_{19}H_{33}$OBr) C, H, Br.

**2-(14-(Bromomagnesio)tetradecyl)-5-methylfuran (7).** To Mg (17 mg, 0.68 mmol) and a crystal of iodine in 1.5 mL of THF at 35 °C was added bromide **6** (0.220 g, 0.62 mmol) in 2.5 mL of THF over 3 h via a syringe pump to provide a 0.14 M solution of **7** (93% of theoretical by titration).[15] GC analysis of quenched (10% HCl) **7** shows >99% **10**.

Authentic samples of byproducts from the Grignard reagent generation (**10-13**) were prepared as follows: To Mg (14 mg, 0.55 mmol) in 1.5 mL of THF at 50 °C was added 1,2-dibromoethane (10 $\mu$L). After 5 min, bromide **6** (0.179 g, 0.50 mmol) in 1 mL of THF was added dropwise, and the reaction mixture was stirred for 1 h at 60 °C. The Grignard was quenched in 10% HCl and extracted into ether. Flash chromatography afforded 61 mg (44%) of **10**, 8 mg (6%) of **11**, 44 mg (16%) of a 5:1 mixture of **13** to **6**, and 50 mg (34%) of **12**.

**5-Methyl-2-tetradecylfuran (10):** $^1$H NMR (400 MHz) 5.83 (br s, 2), 2.55 (t, 3, $J$ = 7), 2.25 (s, 3), 1.63−1.57 (m, 2), 1.25 (br s, 24), 0.88 (t, 3, $J$ = 7); $^{13}$C NMR 154.8, 150.0, 105.7, 105.0, 31.9, 29.7 (4 C), 29.6 (2 C), 29.4 (2 C), 29.3, 28.2, 28.1, 22.7, 14.1, 13.5; IR (neat) 2910, 1470, 800; MS (EI, 10 eV) $m/z$ (relative intensity) 278 ($M^+$, 100); GC $t_R$ 3.46 min. Anal. ($C_{19}H_{34}$O) C, H.

**5-Methyl-2-(tetradec-13-en-1-yl)furan (11):** $^1$H NMR (400 MHz) 5.83−5.78 (m, 3), 5.00 (br d, 1, $J$ = 17), 4.93 (br d, 1, $J$ = 10), 2.55 (t, 2, $J$ = 7), 2.25 (s, 3), 2.04 (q, 2, $J$ = 7), 1.63−1.87 (m, 2), 1.25 (br s, 3); $^{13}$C NMR 129.0, 114.1, 105.7, 105.0, 33.8, 29.6 (3 C), 29.5 (2 C), 29.4, 29.2 (3 C), 28.9, 28.1, 27.9, 13.5 (missing 2 C); IR (neat) 2910, 990, 910; MS (EI, 10 eV) $m/z$ (relative intensity) 276 ($M^+$, 100); GC $t_R$ 3.18 min. Anal. ($C_{19}H_{32}$O) C, H.

**5-Methyl-2-(14-hydroxytetradecyl)furan (12):** $^1$H NMR (400 MHz) 5.83 (s, 3), 3.64 (t, 2, $J$ = 7), 2.55 (t, 2, $J$ = 7), 2.25 (s, 3), 1.63−1.55 (m, 2), 1.26 (br s, 24); $^{13}$C NMR 154.8, 150.0, 105.7, 105.0, 63.1, 32.8, 29.6 (4 C), 29.5, 29.4 (2 C), 29.2, 28.1 (2 C), 25.7, 13.5. IR (neat) 3400, 2910, 2850, 1470, 800; MS (EI, 10 eV) $m/z$ (relative intensity) 294 ($M^+$, 100); GC $t_R$ 5.86 min. Anal. ($C_{19}H_{34}O_2$) C, H.

**1,28-Bis(2-(5-methylfuranyl))octaeicosane (13).** The data for **13** were determined from the mixture: $^1$H NMR (400 MHz) 5.83 (br s, 4), 2.55 (t, 4, $J$ = 7), 2.25 (s, 6), 1.25 (br s, 56); $^{13}$C NMR 154.8 (2 C), 150.0 (2 C), 105.7 (2 C), 105.0 (2 C), 29.7 (7 C), 29.6, 29.5 (2 C), 29.4, 29.2, 28.2, 28.1, 13.5 (2C); IR (neat) 2910, 2850, 1470, 800; HRMS calcd for $C_{38}H_{67}O_2$ 555.5141 (M + H), found 555.5129; GC $t_R$ 19.1 min.

**5-Methyl-2-pentadecylfuran (8).** To Grignard reagent **7** (0.7 mL of 0.30 M, 0.21 mmol) in 0.9 mL of THF at room temperature was added MeI (60 mg, 0.42 mmol) followed by $Li_2CuCl_4$ (0.21 mL of 0.1 M, 0.02 mmol). After 2 h, 10% HCl was added and the resultant solution was extracted into ether. Evaporation in vacuo followed by flash chromatography afforded **8** (42 mg, 68%): $^1$H NMR (400 MHz) 5.83 (s, 3), 3.64 (t, 2, $J$ = 7), 2.55 (t, 2, $J$ = 7), 2.25 (s, 3), 1.63−1.55 (m, 2), 1.26 (br s, 26); $^{13}$C NMR 154.8, 150.0, 105.7, 105.0, 63.1, 32.8, 29.6 (4 C), 29.5 (2C), 29.4 (2 C), 29.2, 28.1 (2 C), 25.7, 13.5; IR (neat) 3400, 2910, 2850, 1470, 800; MS (EI, 10 eV) $m/z$ (relative intensity) 294 ($M^+$, 100); GC $t_R$ 3.33 min. Anal. ($C_{19}H_{34}O$) C, H.

**Palmitic Acid (4).** To $NaIO_4$ (0.21 g, 0.98 mmol) and $RuCl_3$ (5 mg) in 1 mL of 1:1 acetonitrile/water was added furan **8** in 1.6 mL of THF. After 10 min the green-brown mixture was filtered through silica with hexanes followed by 2:1:0.1 hexanes/EtOAc/AcOH to afford palmitic acid (**4**) (41 mg, 67%).

**Radiochemical Synthesis.** The remote gantry system used to prepare [$^{11}$C]methyl iodide has been described.[11] [$^{11}$C]-Carbon dioxide was produced by the $^{14}$N(p,$\alpha$)$^{11}$C nuclear reaction and trapped under vacuum in a copper coil cooled with liquid nitrogen. The trap was warmed to room temperature, and the [$^{11}$C]carbon dioxide was bubbled through $LiAlH_4$ in ether (1.0 M, 0.1 mL) for 3−5 min. The ether was evaporated by bubbling nitrogen through the solution. Aqueous HI (57%, 1.2 mL) was added to the [$^{11}$C]methanol and the vessel heated

to 95 °C. The [$^{11}$C]methyl iodide was distilled via a stream of nitrogen through a drying tube filled with NaOH pellets and $P_2O_5$ powder and trapped by bubbling through THF (0.7 mL) at 0 °C in a 5-mL conical vial.

After the desired activity had been collected, the 0 °C bath was removed and Grignard reagent **7** (0.7 mL of 0.3 M, 0.21 mmol) was added. The mixture was warmed (45 s in a 95 °C bath) and allowed to react at ambient temperature for 5 min. The reaction mixture was removed from the gantry and analyzed by HPLC (Waters Fatty Acid column, THF/$CH_3CN$/$H_2O$, 20/45/35, 2 mL/min, $t_R$ [$^{11}$C]methyl iodide 2.4 min, $t_R$ 2-[$\omega$-$^{11}$C]pentadecyl-5-methylfuran 11.0 min) to afford levels of incorporation between 75 and 90%.

The THF solution of labeled furan **8b** was added to $NaIO_4$ (210 mg, 0.98 mmol) and $RuCl_3$ (5 mg, 0.02 mmol) in 1 mL of 1:1 $CH_3CN/H_2O$ and allowed to stand at room temperature for 8 min. The dark reaction mixture containing a flocculant precipitate was transferred to a 1.5-cm × 25-cm column packed with 8 g of Chelex 100 resin (100–200 mesh, sodium form, BioRad 143-2832) on top of 5 g of silica gel. The column was eluted with pentane in 8-mL fractions. [$\omega$-$^{11}$C]Palmitic acid was obtained in the second through fifth fractions. Unreacted [$^{11}$C]methyl iodide which coelutes with **4d** was removed by evaporation in vacuo. To **4d** redissolved in EtOH (0.7 mL) was added HSA (9 mL, 3% in saline), and the mixture was incubated at 40 °C for 4 min.[13] An injectable solution was prepared by filtration (0.4 and 0.22 $\mu$m Millipore) into a sterile syringe.

Analysis of [$\omega$-$^{11}$C]palmitic acid was performed by HPLC (Whatman Partisil $C_8$, 4.6 × 25 cm, 75% $CH_3CN$ in 0.1% aqueous TFA, 2.0 mL/min, UV at 215 nm and radioactive detector). An ether extract of [$\omega$-$^{11}$C]palmitic acid–HSA complex showed a single radioactive peak (>98% purity) with a retention time ($t_R$ 11.2 min) matching that of [1-$^{11}$C]palmitic acid and palmitic acid. HPLC analysis of the [$\omega$-$^{11}$C]palmitic acid–HSA complex showed the same retention time ($t_R$ 7.4 min) as the [1-$^{11}$C]palmitic acid–HSA complex (Shodex protein analysis column WS-802.5F 8.0 × 300 mm, $H_2O$, 1.0 mL/min).

**Biodistribution Studies.** Female Sprague–Dawley rats (140–160 g, four per time point) were allowed food and water ad lib and were anesthetized with ether just prior to injection. The radiotracer bound to human serum albumin in ethanol–saline[13] was administered via femoral vein injection (≈50 $\mu$Ci/rat). Following 5-, 10-, 15-, 30-, and 60-min intervals, the rats were sacrificed, the tissues were removed and weighed, and the activity levels were determined by $\gamma$-counting.

PET images were obtained from a mongrel dog as previously described.[16]

**Acknowledgment.** We wish to thank Angela A. Beck for preliminary experimental assistance, David R. Marshall for the synthesis of [1-$^{11}$C]palmitic acid, Tammy Pajeau and Henry Lee for the biodistribution studies, and Bill Margenau for cyclotron operation. This work was supported by the National Institutes of Health (PHS 5R01 CA25836 to J.A.K. and PHS 5R01 HL13851 to M.J.W.) and the Department of Energy (DE FG02 86ER60401 to J.A.K. and DE FG02 93ER61659 to S.R.B.).

## References

(1) Presented in part at The Society of Nuclear Medicine 40th Annual Meeting, Toronto, Ontario, Canada, June 8–11, 1993. See abstract in *J. Nucl. Med.* **1993**, *34*, 79P.

(2) (a) Rinaldo, P.; O'Shea, J. J.; Coates, P. M.; Hale, D. E.; Stanley, C. A.; Tanaka, K. Medium-Chain Acyl-CoA Dehydrogenase Deficiency. *N. Eng. J. Med.* **1988**, *319*, 1308–13. (b) Van Hove, J. L. K.; Zhang, W.; Kahler, S. G.; Roe, C. R.; Chen, Y.-T.; Terada, N.; Chace, D. H.; Iafolia, A. K.; Ding, J.-H.; Millington, D. S. Medium-Chain Acyl-CoA Dehydrogenase (MCAD) Deficiency: Diagnosis by Acylcarnitine Analysis in Blood. *Am. J. Hum. Genet.* **1993**, *52*, 958–966. (c) Kelly, D. P.; Mendelsohn, N. J.; Sobel, B. E.; Bergmann, S. R. Detection and Assessment by Positron Emission Tomography of a Genetically Determined Defect in Myocardial Fatty Acid Utilization (Long-Chain Acyl-CoA Dehydrogenase Deficiency) *Am. J. Cardiol.* **1993**, *71*, 738–744. (d) Stanley, C. A.; Hale, D. E.; Coates, P. M. In *Fatty Acid Oxidation: Clinical, Biochemical and Molecular Aspects;* Tanaka, K.; Coates, P. M., Eds.; Liss: New York, 1990; pp 291–302. (e) Roe, C. R.; Coates, M. In *The Metabolic Basis of Inherited Disease;* 6th ed.; Scriver, C. R., Beaudet, A. L., Sly, W. S., Valle, D., Eds.; McGraw-Hill: New York, 1989; Vol. 1, pp 889–914 and references cited therein.

(3) (a) Schelbert, H. R. Features of Positron Emission Tomography as a Probe for Myocardial Chemistry. *Eur. J. Nucl. Med.* **1986**, *12*, S2–S10. (b) Schelbert, H. R. Assessment of Myocardial Metabolism by PET - A Sophisticated Dream or Clinical Reality? *Eur. J. Nucl. Med.* **1986**, *12*, S70–S75. (c) Saha, G. B.; Go, R. T.; MacIntyre, W. J. Radiopharmaceuticals for Cardiovascular Imaging *Nucl. Med. Biol.* **1992**, *19*, 1–20. (d) Schwaiger M.; Hicks, R. The Clinical Role of Metabolic Imaging of the Heart by Positron Emission Tomography. *J. Nucl. Med* **1991**, *32*, 565–578 (e) Bergmann, S. R., Sobel, B. E., Eds. *Positron Emission Tomography of the Heart*; Futura Publishing Co, Inc.: New York, 1992.

(4) Pochapsky, S. S.; VanBrocklin, H. F.; Welch, M. J.; Katzenellenbogen, J. A. Synthesis and Tissue Distribution of Fluorine-18 Labeled Trifluorohexadecanoic Acids. Considerations in the Development of Metabolically Blocked Myocardial Imaging Agents. *Bioconj. Chem.* **1990**, *2*, 231–244.

(5) Kihlberg, T.; Malmborg, P.; Långström, B. Syntheses of [$\omega$-$^{11}$C]-Labeled Fatty Acids Using Alkyl Halides and Grignard Reagents. *J. Labelled Comp. Radiopharm.* **1991**, *30*, 151–152.

(6) Carlsen, P. H. J.; Katsuki, T.; Martin, V. S.; Sharpless, K. B. A Greatly Improved Procedure for Ruthenium Tetraoxide Catalyzed Oxidations of Organic Compounds. *J. Org. Chem.* **1981**, *46*, 3936–3938.

(7) Büchi, G.; Wüest, H. An Efficient Synthesis of *cis*-Jasmone. *J. Org. Chem* **1966**, *31*, 977–988.

(8) Lai, Y.-H. Grignard Reagents from Chemically Activated Magnesium. *Synthesis* **1981**, 585–604.

(9) Schlosser, M. Prescriptions and Ingredients for Controlled CC Bond Formation with Organometallic Reagents. *Angew. Chem., Int. Ed. Engl.* **1974**, *13*, 701–706.

(10) Rieke, R. D. Preparation of Highly Reactive Metal Powders and Their Use in Organic and Organometallic Synthesis. *Acc. Chem. Res.* **1977**, *10*, 301–306.

(11) Tamura, M.; Kochi, J. Coupling of Grignard Reagents with Organic Halides. *Synthesis* **1971**, 303–305.

(12) Dence, C. S.; Lechner, K. R.; Welch, M. J. Remote System for the Routine Production of [$^{11}$C]-Methyl Albumin. Application to Pulmonary Studies. *J. Labelled Comp. Radiopharm.* **1993**, *32*, 174–175.

(13) Welch, M. J.; Dence, C. S.; Marshall, D. R.; Kilbourn, M. R. Remote System for Production of Carbon-11 Labeled Palmitic Acid. *J. Labelled Comp. Radiopharm.* **1983**, *20*, 1087–1095.

(14) (a) Chance, E. M.; Seeholzer, S. H.; Kobayashi, K.; Williamson, J. R. Mathematical Analysis of Isotope Labeling in the Citric Acid Cycle with Applications to $^{13}$C NMR Studies in Perfused Rat Hearts. *J. Biol. Chem.* **1983**, *258*, 13785–13794. (b) Neurohr, K. J.; Barrett, E. J.; Shulman, R. G. In Vivo Carbon-13 Nuclear Magnetic Resonance Studies of Heart Metabolism. *Proc. Natl. Acad. Sci. U.S.A.* **1983**, *80*, 1603–1607. (c) Sherry, A. D.; Malloy, C. R. Studies of Intermediary Metabolism in the Heart by $^{13}$C NMR Spectroscopy. In *NMR Techniques in the Study of Cardiovascular Structure and Function*; Osbakken, M., Haselgrave, J., Eds.; Futura Publishing Co., Inc.: Mount Kisco, NY, 1988; pp 272–287.

(15) Watson, S. C.; Eastham, J. F. Colored Indicators for Simple Direct Titration of Magnesium and Lithium Reagents. *J. Organomet. Chem.* **1967**, *9*, 165–168.

(16) Brown, M. A.; Myears, D. W.; Bergmann, S. R. Noninvasive Assessment of Canine Myocardial Oxidative Metabolism with Carbon-11 and Positron Emission Tomography. *J. Am. Coll. Cardiol.* **1988**, *12*, 1054–1063.